Declaration page for the Masters of Research thesis

This thesis is written in the form of a journal article for **The Journal of Comparative Neurology**

Declaration

All research described in this report is my own original work.

This work has not been submitted for a higher degree to any other university or institution.

Zachary Sheehan

6/10/17

Differential investment in brain regions of polymorphic diurnal and nocturnal *Myrmecia* ants

Zachary Sheehan

Department of Biological Sciences, Macquarie University

Contents

Acknowledgements

I would of course like to acknowledge the support of my supervisor Ajay Narendra, who helped me every step of the way, opened me up to so much knowledge and opportunities, and perhaps most important of all, was actually willing to support me all throughout this project. I also thank Franne Kamhi for all of your help and support. You probably bore the brunt of most of my questions, complaints, struggles etc. and you taught me so many skills that I couldn't have completed this project without. I would also like to thank everyone else in our lab group; Yuri, Ravi and Duncan. Your wealth of knowledge and reassurance when things were tough were helpful beyond belief. Whether it be answering my inane questions, spending an entire day watching ants or just everyday conversation, your attitude and presence alone made everything more enjoyable.

I would like to thank the Macquarie University Microscopy Department for access to their facilities and their support throughout this project. This project would have literally been impossible without them.

I would also like to thank my family for supporting me this past few months, despite them seeing or hearing even less of me than usual. Yes, I am still alive and thank you.

And lastly I would like to thank my MRes cohort who have, in a way, become like family. Over the past months you alone have had to deal with most of my struggles, complaints, highs and lows, just as I have had to deal with yours. Most of us were strangers when we started but I imagine this entire experience would have less without you and I am glad to have made as good friends as you.

Abstract

Many nocturnal insects have evolved optical adaptations to capture more light at night but these adaptations are not sufficient to explain visually guided behaviour seen at night. Hence, there must be additional neural adaptations to explain this behaviour. At the same time, the size of brain neuropil can be significantly constrained by the size of the animal. Here, I asked if the size of functionally distinct brain regions change in two congeneric polymorphic bull ants, the diurnal *M. gulosa* and the nocturnal *M. midas*. I took advantage of the extreme intraspecific size range in both species to also ask how body size affects brain region scaling. I found that the diurnal species invests more into the optic lobes, while the night-active species invests more into the antennal lobes and mushroom bodies, in complete contrast with predictions. The higher order processing neuropils of the central complex did not differ significantly between species, except in the central body lower. I also found neuropil volume changes as body size changes, with larger individuals having larger neuropils and smaller individuals having smaller neuropils. These results show that there are adaptations in the brains of diurnal and nocturnal bull ants that may help with activity in different temporal niches and that the volume of these regions does not exist independently from size.

Key Words

Myrmecia, temporal niche, optic lobe, antennal lobe, mushroom body, central complex, scaling

Introduction

Insects occupy different temporal niches (Nakadai & Kawakita, 2017; Narendra, Greiner, Ribi, & Zeil, 2016) and the ability to navigate back and forth between places of significance, such as food sources, nests and habitats, is a fundamental requisite for almost all activity (Wolf, 2011). For this insects must sense the world, with the vast majority of them relying on olfaction, vision, mechanoreception and magnetoreception (Duggan, García-Añoveros, & Corey, 2000; Hansson & Stensmyr, 2011; Vacha, 2006; Wystrach, Dewar, & Graham, 2014). These sensory modalities require external sensory structures along with relevant information processing and integration centres in order to be functionally useful (expect for magnetoreception which has only been described in a few insects and as yet has no specific structures described in any animal). These structures are heavily influenced by body size because as an animal gets smaller, surface area and volume also decrease which can in turn dictate the size and number of these sensory structures that an animal may support. (Narendra, Kamhi, & Ogawa, 2017; Ramirez-Esquivel, Zeil, & Narendra, 2014). In addition, for insects relying on vision, the time at which they are active also plays a crucial role in detecting information and subsequently in processing and integrating of sensory information (Narendra et al., 2017).

Many groups show variation in body size and occupy different temporal niches but analysis and understanding the effects of these are often hampered by phylogenetic constraints. Ants are a useful model to investigate how sensory structures and regions change because there is great size variation both between and within species. In addition, closely related animals often occupy different temporal niches (Ilieş, Muscedere & Traniello, 2015; Narendra et al., 2017). Having such variation within even the same species, are particularly suited to exploring these types of questions. We know that both the number of antennal sensilla and facet numbers increase with body size (Narendra et al. 2017; Ramirez-Esquivel et al., 2014). However, irrespective of their size, ants active at low light levels tend to have larger lenses and wider photoreceptors to maximise photon capture (Narendra et al. 2017). Both diurnal and nocturnal *Myrmecia* ants rely heavily on vision for hunting prey and for navigation (Freas, Narendra, Lemesle, & Cheng, 2017; Jayatilaka, Raderschall, Narendra, & Zeil, 2014). To operate in low light habitats, the nocturnal ants have evolved exquisite optical adaptations that include large lenses and wide rhabdoms to gather more light (Narendra et al. 2017). These optical adaptations alone are not sufficient to explain the visually guided behaviour of animals in dim

light. Hence it is of interest to identify whether there are clear volumetric differences in the sensory processing brain regions between day and night-active animals.

Ant brains have a number of functionally distinct brain regions that process different types of sensory and motor functions (Fig.1). They have optic lobes which are responsible for initial processing of visual information coming from the eye and are comprised of three main regions: the lamina, medulla and lobula (Meyer, Matute, Streit, & Nässel, 1986). In the optic lobe there is a small neuropil known as the accessory medulla and it appears to be involved in circadian timekeeping functions (Loesel & Homberg, 2001). The antennal lobes are responsible for processing olfactory as well as some tactile information (Hansson, Anton, & Christensen, 1994; Hansson & Anton, 2000). The mushroom bodies are an important structure in the insect brain associated with learning, memory and sensory integration (Farris, 2005) and that can be separated into three different regions: the calyx, pedunculus and the lobes. In Hymenopterans the calyx can be further divided into the basal ring, lip and collar with the lip and collar associated specifically with olfactory and visual information respectively (Krofczik, Khojasteh, de Ibarra & Menzel, 2008; Seid & Wehner, 2008). An important region in the insect brain is the central complex. It has been associated with a number of functions including visual information processing during flight, spatial orientation, visual memory, locomotion, (Homberg, Heinze, Pfeiffer, Kinoshita & el Jundi, 2011; Neuser, Triphan, Mronz, Poeck, & Strauss, 2008; Strauss, 2002) Other regions in the brain include the subesophageal ganglion, which has been mainly associated with mandible control (Maeda, Tamotsu, Iwasaki, Nisimura, Shimohisigashi, Hojo & Ozaki 2014), the anterior optic tubercle, which is a major target of visual interneurons from the optic lobe and is involved in the polarised light pathway (Homberg, Hofer, Pfeiffer, Gebhardt, 2003; Schmitt, Stieb, Wehner, Rössler, 2016) and the remainder of the central brain/protocerebrum, whose role in the brain is currently unclear. While ant brains have been well characterised (Gronenberg, Heeren, & Hölldobler, 1996; Kubota, Tsuji, Misaka, Yokohari, & Nishikawa, 2006; Stieb et al., 2010), to the best of my knowledge there has been no comparisons of brains between day- and night-active ants. Most of our knowledge in this field comes from studies on hawkmoths (Stöckl, Heinze, Charalabidis, el Jundi, Warrant & Kelber, 2016a; Stöckl, Ribi, & Warrant, 2016b) and dung beetles (Immonen, Dacke, Heinze, & El Jundi, 2017) which show that nocturnal species have adaptations for activity at night. When compared with a diurnal relative, nocturnal hawkmoths invest more into their antennal lobes and less into their optic lobes. In the dung beetles, the antennal lobes were indistinguishable between nocturnal

and diurnal species. In the optic lobes, only the lamina showed any significant difference, with the nocturnal species investing more into the lamina.

Ants can show significant variation in body size both within and between species. Distinct castes with morphological differences are a key feature of this group and these morphological differences may also affect the brain (Ilieş et al. 2015; Narendra et al. 2017). As size increases and decreases, the amount of space available to the brain and to sensory structures such as eyes and antennae changes. This means there can sometimes be significant relationships between the size of an ant and the size of its brain. In general, larger ants appear to have larger brains and they display allometric scaling (Gronenberg, Heeren, & Hölldobler, 1996; Kühn-Bühlmann & Wehner, 2006; Muscedere & Traniello, 2012; Seid, Castillo, & Wcislo, 2011; Stieb, Muenz, Wehner, & Rössler, 2010). The larger body size means larger sensory structures and a larger brain to process this increase in brain size. A similar result is found as ants get smaller, with brain size also reducing. However, factors such as the age of an ant, its experiences, its species and its caste can all influence this brain scaling relationship (Gronenberg et al. 1996; Kühn-Bühlmann et al. 2006; Muscedere et al. 2012). Workers of the genus *Atta* have been shown to have diphasic brain scaling relationships between large and small workers with brain size scaling significantly differently between the two (Seid et al. 2011). As with bees, it has also been shown that as an ant gets older and gains new experiences certain parts of the brain may grow or reduce in size, this in turn can lead to more differences in scaling relationships between different ants, even within the same colony (Gronenberg et al. 1996).

However, in the breadth of these studies there has been no exploration of the effect of a diurnal and nocturnal lifestyle on the scaling of the ant brain and individual regions across different size ranges. Here, I studied two congeneric species of bull ants (*Myrmecia*) which are polymorphic, with *M. gulosa* active during the day and *M. midas* active mostly during night. I carried out a volumetric analysis of different functionally distinct brain regions to determine the effect time of activity and body size. Here I asked if there were any significant differences in the volume of the brain and/or brain regions between the two species and if the volume of the brain and/or brain regions is affected by size. I hypothesised that there would be differences in the brains of the two species due to their adaptation to different temporal niches and that their brain volumes would differ depending on their body

size. Due to the relatively limited amount of light available at night I predicted that the night active *M. midas* would invest more into visual information processing than *M. gulosa*. This would mean that regions such as the optic lobe and the collar of the mushroom bodies would be larger in *M. midas* and *M. gulosa*. I also predicted that the other brain regions would show a similar level of investment in both species due to the relatively similar ecological niche and behavioural repertoire of the two species. In the case of body size I predicted that individuals with a smaller body size would in turn show a smaller brain volume and a larger brain volume for larger sized individuals. These size differences would also be seen for each of the individual brain regions rather than just the entire brain as a whole.

Materials and Methods

Study Species

Here I studied two species of bull ants *Myrmecia gulosa* (Fabricius, 1775) and *Myrmecia midas* (Clark, 1951) (Fig.2). *M. gulosa* workers were collected from five nests at the Hawksbury campus of Western Sydney University, Sydney, Australia (33°47'40.7'' S, 150° 45'41'' E). *M. midas* workers were collected from six nests on the Macquarie University North Ryde campus, Sydney, Australia (33°46'11'' S, 151°6'39.4'' E). These ants were collected from around the nest entrance, the nests were not dug up for collection. All ants were transported to Macquarie University, fed with sugar solution and dissected within 48 hours. A total of 83 *M. gulosa* workers from 5 nests and a total of 107 *M. midas* workers from 5 nests were collected.

Activity Schedule

To identify the activity schedule of these species I monitored one nest of *M. gulosa* on 20 April 2017, from before sunrise until after sunset. I set up a 60cm diameter reference perimeter around the nest entrance and recorded the time of departure and arrival through this perimeter. I observed ants at low light levels using a head lamp with a red filter. This appeared to not affect their behaviour. For *M. midas*, their activity schedule was recently described from the same study site (Freas, Narendra, & Cheng, 2017) and I used these results.

Synapsin Immunolabelling

Synapsins are a group of proteins expressed in presynaptic terminals where they are involved in regulating neurotransmitters. They are believed to bind to synaptic vesicles and control the release of neurotransmitters into a synapse (Evergren, Benfenati, Shupliakov, 2007). Expression of synapsin in invertebrates is highly conserved and thus useful for examining insect brain anatomy. To label synaptic neuropils in wholemounts I used anti-synapsin antibodies. The specificity of SYNORF1 has been demonstrated in *Drosophila* synapsin mutants which showed altered synapsin labelling (Godenschwege et al., 2004). It has also been used to identify synaptic neuropils in ants (Seid & Junge, 2016; Bressan et al. 2014; Groh et al. 2014) as well as several other insects including honeybees (Brandt et al., 2005), locusts (Leitinger, Pabst, Rind, & Simmons, 2004), dung beetles (Immonen et al. 2017), moths (Stockl, et al. 2016a), butterflies (Montgomery & Ott, 2015) and cockroaches (Wei, el Jundi, Homberg, & Stengl, 2010).

The protocol I have used here was modified from Muscedere & Traniello (2012). Before dissection, animals were cooled on ice and imaged from the dorsal view using a Panasonic MC-F21000 camera. All 83 *M. gulosa* workers and 107 *M. midas* workers were used for head measurements. The head width (HW) of each ant was measured from the image, taken from the dorsal view, along the widest point of the head, directly behind the eyes. Ants were then dissected in cooled saline solution (129 mM NaCL, 6 mM KCl, 4.3 mM $MgCl_2$ x $6H_20$, 5 mM $CaCl_2$ X $2H_20$, 159.8 mM Sucrose, 274 mM D-glucose, 10 mM HEPES buffer, pH 6.7) and immediately transferred into the fixative, (4% paraformaldehyde in phosphate buffered saline [PBS]) for two days at room temperature. The brains were then washed in PBS (3 x 10 minutes). For permeabilising the tissue, the brains were incubated in 3% Triton-X in PBS (PBST; 3 x 10 minutes). This was followed by incubation of the brains in 2% Normal Goat Serum (NGS; Sigma-Aldrich) and PBST for one hour at room temperature. Samples were then transferred to the primary antibody 3C11 anti-SYNORF1 (1:50, DHSB; see Table 1) with 2% NGS in PBST and incubated for four days on a shaker at room temperature. Following further PBS washes (5 x 10 minutes), specimens were transferred to the secondary antibody (Alexa Fluor 488 [Merck], 1:250; with 1% NGS in PBST) and kept in the dark for three days at room temperature on a shaker. Antibody incubation was followed by PBS washes (5 x 10 minutes) and dehydration using an increasing ethanol series (30%, 50%, 70%, 90%, 95%, 100%, 100%; 10 minutes each). The brains were then transferred into 100% methyl salicylate and incubated one hour on a shaker at room temperature.

Custom made metal slides with 1 cm diameter holes were sealed on one side by gluing on a coverslip to create a well. Brains were transferred to the slides, with the ventral side facing upwards, and immersed in 100% methyl salicylate. Slides were then sealed with a coverslip and left overnight to allow any excess methyl salicylate on the slides to evaporate. All *M. gulosa* and *M. midas* individuals were processed using this protocol but only 31 *M. gulosa* and 28 *M. midas* resulted in clear enough images for accurate volumetric measurements.

Brain Labelling

The wholemount brains were imaged using an inverted confocal laser scanning microscope (Olympus FluoView FV1000© IX81). I used a 10x objective and optically sectioned the brain of all animals at 3.1 μm. Due to the large size of the bull ant brain, three overlapping z-stacks were imaged: one of the central brain and one for each of the optic lobes. Subsequently, I used Amira (v. 6.0.1, FEI Visualization Sciences Group, Düsseldorf, Germany) to trace functionally distinct neuropils, obtain volumetric measurements and create 3D reconstructions. I traced the following well defined regions in the ant brain (Fig.1,3): the antennal lobes (AL), mushroom bodies (MB), containing the lip (CA-Lip, collar (CA-Collar) and peduncle (PE). The optic lobes (OL), containing the lamina (LA), medulla (ME) and lobula (LO). The central complex (CX), containing the central body upper (CBU), the central body lower (CBL), the noduli (NO) and the protocerebral bridge (PB). Finally, I also traced the subesophageal zone (SEZ) and the remainder of the central brain (ROCB). The accessory medulla and the anterior optic tubercle were not traced because it was not possible to obtain images of these regions that were clear enough for volumetric analysis. One hemisphere was traced for all brain regions except for the CX and SEZ because of their location in the central brain. The volume of the regions only traced in one hemisphere were doubled to estimate the volume of these regions in the entire brain. 'Whole Brain' measurements were also obtained by summing the volumes of all brain neuropils. To trace a brain region, I identified where the particular region first appeared in the image stack and then used the 'Brush' tool to outline the bounds of the region. I then moved four slices deeper into the image stack and did the same. I repeated this process until I reached where the particular region ended in the stack. I then used the 'Interpolate' function to trace the region in the images slices I did not trace. I then went through each image slice and ensured the interpolation worked correctly, cleaning up any mistakes using the 'Brush' tool. I repeated this same procedure for all of the brain

regions in each ant. For the SEZ, a region whose boundaries are often difficult to define, I carefully traced the neuropil slice-by-slice, observing the boundaries as I went in order to clearly differentiate it from the other brain neuropils. To get volumetric measurements I used the 'Material Statistics' function and to obtain 3D-resconstrutions I used the 'Generate Volume' function.

Statistical Analysis

I first identified whether there was a nest effect in each species using a linear model in R (RCoreTeam, 2017). 'Nest effect' being any significant difference in brain volume that appeared to occur only in an individual nest or nests. These effects may be due to varying phylogenetic or environmental factors and would influence interpretation of the results. The linear model also allowed me to determine how well any variance in the data could be explained by two main variables of interest: HW and species. Multiple models were tested to explore which would best explain the variance in the data. The most effective model was a combination of both HW and species.

Both species exhibit extreme body size variation. Hence I carried out a scaling analysis (SMA) to test the relationship between different brain regions and body size. For this, I performed a standardised major axis (SMA) regression in R using the statistical package (S)MATR v. 3.4 (Warton, Wright, Falster, Westoby, 2006;Warton, Duursma, Falster, & Taskinen, 2012) which reduces the data of the two groups into two slopes which are then statistically compared. I was interested in determining if, across HW, there was a significant grade shift between the two species for a particular region. Tests for grade shifts could only be carried out if the slopes for the two groups were not significantly different, which was the case for all brain regions. All variables were natural log-transformed before analysis. I also used two-sample t-tests to determine if there were any significant differences in the relative volume of particular regions, between the day-active and night-active species. The data used for the t-tests were normally distributed (Shapiro-Wilk normality test).

Results

Activity schedule

M. gulosa foragers left the nest around 10 minutes before sunrise and the last individual returned around 20 minutes after sunset. The number of ants leaving the nest peaked 5-10 minutes before sunrise. A large number of foragers began to return around an hour before midday following which, ants continued to leave and return to the nest intermittently for most of the day. Most individuals returned to the nest in the late afternoon, 10-15 minutes before sunset, with only a few continuing to return in far lower light levels, 10-20 minutes after sunset (Fig.2).

M. midas foragers began leaving the nest in the early evening 10-20 minutes after sunset. Individuals began returning to the nest within 30 minutes and continued to return intermittently over the nest of the night until a final peak inbound activity around 30 minutes after sunrise (Fig.2). Most foragers will have left the nest by around an hour before midnight with only a few individuals leaving again later at night (Freas et al., 2017).

Head width variation

Both *M. gulosa* and *M. midas* showed significant intraspecies size variation. HW of *M. gulosa* varied from 1.9-4.0mm. *M. midas* individuals were slightly larger, with head widths ranging from 2.1-4.5mm (Fig.2). I carried out volumetric measurements for individuals ranging from 1.9-3.8mm in *M. gulosa* and 2.1-4.3mm in *M. midas* (Fig.2).

Variation in brain region volumes

In both species, the size of the OL, AL, MB, and CX did not vary between nests (Table.2). Hence, I combined the data from all nests for both species. Below, I will address how the size of the functionally distinct neuropils change with time of activity and HW.

Whole brain: The scaling analysis indicated that for a given head width, there was no difference in the absolute volumes of all neuropils between *M. gulosa* and *M. midas* (W^2 = 0.00492, p = 0.94408; Table. 4; Fig.3). Overall, the variation in whole brain volumes was best explained by a combination of HW and species (R^2 = 0.2751, *F =10.63, p<0.001; Table 5,6*).

Antennal lobes (AL): Relative to the entire brain, the volume of the AL (Fig. 4) was larger in the nocturnal *M. midas* compared to the diurnal *M. gulosa* (t=-5.7491, p<0.0001; Table. 3; Fig. 4). Similarly, the scaling analysis indicated that for a given HW, the nocturnal *M. midas*

had larger AL compared to the diurnal species (W^2= 12.64, $p < 0.001$; Table. 4; Fig. 4). The variation in the AL volumes was best explained by a combination of both HW and the species (R^2=0.4748, F=25.32, p<0.0001; Table. 5,6)

Optic lobes (OL): Relative to the entire brain, the volume of the OL (Fig. 5) was larger in the diurnal *M. gulosa* compared to the nocturnal *M. midas* (t=6.3493, p<0.0001; Table 3; Fig. 5). This was also true for the lamina (t=6.7727, p<0.0001), medulla (t=6.1322, p<0.0001) and lobula (t=2.6647, p<0.01; Table. 5; Fig. 5). The scaling analysis indicated that for a given HW, the absolute volume of the entire OL and the LA, ME, LO neuropils were smaller in the night-active *M. midas* compared to the day-active *M. gulosa* (W^2= 23.95, $p < 0.0001$; Fig. 5; Table. 4). The variation in the entire OL and the LA, ME, LO neuropils was best explained by both the time of activity and HW (R^2=0.4703, F=24.86, p<0.0001; Table. 5,6). Species was not a significant factor to explain the variation in the lobula (R^2=0.000002, F=0.0013, p=0.97; Table. 5.6).

Mushroom Bodies (MB): Relative to the entire brain, the volume of the MB (Fig. 6) was larger in the nocturnal *M. midas* compared to the diurnal *M. gulosa* (t=-8.7822, p<0.0001; Table. 3). This was also true for the lip (t=-6.0711, p<0.0001), collar (t=-6.7984, p<0.0001) and peduncle (t=-5.0134, p<0.0001; Table. 3). The scaling analysis indicated that for a given HW, the absolute volume of the entire MB and the CA-Lip, CA-Collar, PE neuropils were larger in the night-active *M. midas* compared to the day-active *M. gulosa*. (W^2= 10.07, $p < 0.01$; Table. 4; Fig. 6). The variation in the entire MB and three MB neuropils was best explained by both species and HW (R^2=0.5939, F=40.94, p<0.0001; Table. 5,6).

Central Complex (CX): Relative to the entire brain, the volume of the CX (Fig. 7) was not significantly different between the diurnal *M. gulosa* and the nocturnal *M. midas* (t=-0.91497, p=0.4187; Table. 3) and this was similar for the UU (t=0.3829, p=0.7032), N (t=0.7735, p=0.4431) and PCB (t=-0.94351, p=0.346; Table. 3; Fig. 7). However, the LU was larger in the day-active *M. gulosa* (t=2.4022, p<0.01). The scaling analysis indicated that the absolute volumes of the CX, UU, N and PCB were not different between species. The LU was larger, for a given HW, in the day-active *M. gulosa* compared to the night-active *M. midas* (W^2= 7.428, $p < 0.01$; Table. 4). Neither W nor species significantly explained the variation seen in the CX and four CX neuropils (R^2=0.07822, F=2.376, p=1.022; Table.5,6)

Discussion

In this study, I investigated the differential investment of functionally distinct brain regions in polymorphic diurnal and nocturnal *Myrmecia* ants. I found that the overall brain size did not differ between the diurnal and nocturnal species. The OL were larger in the day-active animals (Fig. 5) and the AL were larger in the nocturnal animals (Fig. 4). In the higher order information processing centres, the MB was larger in the nocturnal ant (Fig. 6). Interestingly, the size of the CX did not change between the diurnal and nocturnal species, with only the CBL of the CX being slightly larger in the day-active ant (Fig. 7). Both head width and species together explained the variance seen in the volumetric measures of all neuropils except the central complex.

Similar to what is seen in hawkmoths (Stöckl et al., 2016a), I found increased investment into the AL by the nocturnal bull ant species and more investment into the OL by the diurnal species (Fig. 4,5). Smaller OL volumes in the nocturnal species may suggest less reliance on visual information but it is also possible that other processes, such as neural summation, may be occurring in the OL. Nocturnal hawkmoths (Stöckl, O'Carroll, & Warrant, 2016;b Stöckl et al., 2016a) and nocturnal bees (Greiner, Ribi, & Warrant, 2004) are suggested to spatially summate information coming from the eye and preliminary studies suggest nocturnal ants may also have similar adaptations (Wood, 2014). This may be why nocturnal ants are able to have smaller OL than their diurnal counterparts.

There were also significant differences in the MB of the two bull ant species that appears to contrast with previous work in other species. The MB of nocturnal and diurnal hawkmoths shows a difference in the calyx and the accessory calyx between the two species (Stöckl et al., 2016a). The ratio of visual versus olfactory region of the calyx also differed in both species. In the dung beetles, however, the mushroom bodies were not significantly different between diurnal and nocturnal species (Immonen et al. 2017). These findings are in contrast to my findings in bull ants, which show that there is significantly more investment into every region of the mushroom bodies in the nocturnal *M. midas* compared with *M. gulosa* (Fig. 6). Given the increase in antennal lobe investment by *M. midas*, corresponding investment into the lip region of the mushroom bodies is unsurprising. But it is also apparent that *M. midas* invests more than *M. gulosa* into every mushroom body region including the collar. It may be that rather than investing as much into the optic lobes as *M. gulosa*, *M. midas* invests more into the integration of these sensory modalities in the mushroom bodies. While *M. gulosa* can

afford to invest significantly into visual information processing, *M. midas* may be combining and integrating visual, olfactory and tactile information to function more effectively in low light levels.

Much like the mushroom bodies, the central complex of the dung beetle showed no significant differences between diurnal and nocturnal animals (Immonen, Dacke, Heinze, & el Jundi, 2017). In the hawkmoths, however, there were some differences, while the NO had no difference between species, there was more investment by the diurnal species in the CBU and more investment into the CBL by the nocturnal species (Stöckl et al., 2016a). In the bull ants the only region that showed any significant difference between species was the CBL and in this case it was the diurnal species that showed more investment (Fig.7). Every other structure in the central complex was similar in volume between species (Fig. 7).

This constancy in central complex volumes also occurs across different HW. For both *M. gulosa* and *M. midas* the volume of the CX and the different regions within (CBU, BCL, NO, PB) do not change with HW (Fig. 7). Linear modelling also shows that HW can explain very little of the variance seen in the CX (Table. 6) These finding further emphasise that the need to navigate efficiently is common across animals of different sizes. My data suggest that there is a given volume of the CX that is sufficient for this. It appears that it is possible the CX cannot be smaller than a certain size and once that size is reached, there is no need to significantly increase any further (Weir & Dickinson, 2015; Seelig & Jayaraman, 2015; Varga, Kathman, Martin, Guo, & Ritzmann, 2017; de Vries, Pfeiffer, Trebels, Adden, Green, Warrant, & Heinze, 2017) and this may explain the limited differences we see in the regions that make up this structure. However, when we examine the slopes for this region we see that the CX neuropil volumes appear to scale allometrically with HW (Table. 6,7). This indicates that there may still some level of positive allometric scaling in the CX of these species. However, due to the limited amount of variance that can be explained by size in this region it is not possible to make definite conclusions about the scaling of this region. Alongside simple volume changes it is also plausible that the neuronal connections within the central complex change with HW or between day and night, and this needs to be examined in future studies.

The relationship between HW and all other brain neuropils appears to be similar in both species. With larger *M. gulosa* individuals and larger *M. midas* individuals generally having larger neuropils. As animals increase in size, not only does their body get larger, so does the size of their sensory structures and therefore larger sensory and motor brain regions are

needed. This may explain why there is an increase in neuropil volumes as size increases in these two species. For all of these neuropils the data also appears to indicate a positive allometric relationship between neuropil volume and HW (Table. 6,7). This suggests that though the volume of these regions scale with HW, they do not scale isometrically. Instead it appears that as HW increases, the volume of these brain regions increases more significantly than a simple one-to-one ratio. This may indicate that as HW increase there is a significant increase in the amount of processing power required by the brain to function. The increase in sensory structure size would require equivalent processing but the complexity of processing may mean that an isometric increase in neuropil volume is inadequate for an ants processing needs. Similarly, at the smaller scale, the sensory structures of smaller ants (due to their size) may require far less tissue for processing than larger ants and may explain the trend to far smaller brain in these smaller individuals.

While both head width and time of activity best explained the size variation of most neuropils, they did not explain most of the variance. Some brain regions, such as the mushroom bodies, change with age and experience (Gronenberg et al., 1996; Kühn-Bühlmann & Wehner, 2006; Muscedere & Traniello, 2012; Stieb et al., 2010), two factors that were not controlled for in this study. It is possible that these, and other neuropils, may be subject to such factors and this may explain the variance seen in the neuropil volumes of these bull ants.

Conclusion

In this study, I have described quantitative differences in bull ant brain morphology across species and body size. I have found that diurnal and nocturnal bull ant species invest differentially into brain neuropils suggesting potential adaptations to their ecological niche. I also found that body size may play a role in the volume of these regions, at least for the diurnal species. The results of this study will be valuable in interpreting past and future quantitative neuroanatomical studies of ants and insects in general, as this study relied on a large dataset, and provides the first in depth comparison of diurnal and nocturnal ant brains.

References

Brandt, R., Rohlfing, T., Rybak, J., Krofczik, S., Maye, A., Westerhoff, M., . . . Menzel, R. (2005). Three-dimensional average-shape atlas of the honeybee brain and its applications. *The Journal of Comparative Neurology, 492*(1), 1-19. doi:10.1002/cne.20644

Bressan, J. M. A., Benz, M., Oettler, J., Heinze, J., Hartenstein, V., & Sprecher, S. G. (2014). A map of brain neuropils and fiber systems in the ant *Cardiocondyla obscurior*. *Frontiers in Neuroanatomy*, 8, 166. doi:10.3389/fnana.2014.00166

Clark, J. (1951). *The Formicidae of Australia. vol. 1. Subfamily Myrmeciinae* (Vol. 1). Melbourne, Vic: CSIRO.

Duggan, A., García-Añoveros, J., & Corey, D. P. (2000). Insect mechanoreception: What a long, strange TRP it's been. *Current Biology, 10*(10), R384-R387. doi:10.1016/S0960-9822(00)00478-4

Evergren, E., Benfenati, F., Shupliakov, O. (2007). The synapsin cycle: a view from the synaptic endocytic zone. *Journal of Neuroscience Research* 85 (12): 2648–56. doi:10.1002/jnr.21176. PMID 17455288.

Fabricius, J. C. (1775). *Systema entomologiae, sistens insectorum classes, ordines, genera, species, adjectis synonymis, locis, descriptionibus, observationibus*: Kort.

Farris, S. M. (2005). Evolution of insect mushroom bodies: old clues, new insights. *Arthropod Structure & Development, 34*(3), 211-234. doi:https://doi.org/10.1016/j.asd.2005.01.008

Freas, C. A., Narendra, A., & Cheng, K. (2017). Compass cues used by a nocturnal bull ant, *Myrmecia midas*. *Journal of Experimental Biology, 220*(9), 1578-1585. doi:10.1242/jeb.152967

Freas, C. A., Narendra, A., Lemesle, C., & Cheng, K. (2017). Polarized light use in the nocturnal bull ant, *Myrmecia midas*. *Royal Society Open Science, 4*(8), doi:10.1098/rsos.170598

Godenschwege, T. A., Reisch, D., Diegelmann, S., Eberle, K., Funk, N., Heisenberg, M., . . . Buchner, E. (2004). Flies lacking all synapsins are unexpectedly healthy but are impaired in complex behaviour. *European Journal of Neuroscience, 20*(3), 611-622. doi:10.1111/j.1460-9568.2004.03527.x

Greiner, B., Ribi, W., & Warrant, E. (2004). Retinal and optical adaptations for nocturnal vision in the halictid bee *Megalopta genalis*. *Cell and Tissue Research, 316*(3), 377-390. doi:10.1007/s00441-004-0883-9

Groh, C., Kelber, C., Grübel, K., & Rössler, W. (2014). Density of mushroom body synaptic complexes limits intraspecies brain miniaturization in highly polymorphic leaf-cutting ant workers. *Proceedings of the Royal Society B: Biological Sciences*, 281(1785), 20140432. doi:10.1098/rspb.2014.0432

Gronenberg, W., Heeren, S., & Hölldobler, B. (1996). Age-dependent and task-related morphological changes in the brain and the mushroom bodies of the ant *Camponotus floridanus*. *Journal of Experimental Biology, 199*(9), 2011-2019.

Hansson, B., Anton, S., & Christensen, T. (1994). Structure and function of antennal lobe neurons in the male turnip moth, *Agrotis segetum* (Lepidoptera: Noctuidae). *Journal of Comparative Physiology A, 175*(5), 547-562. doi:10.1007/BF00199476

Hansson, B. S., & Anton, S. (2000). Function and morphology of the antennal lobe: New developments *Annual Reviews in Entomolology* (Vol. 45, pp. 203-231).

Hansson, B. S., & Stensmyr, M. C. (2011). Evolution of insect olfaction. *Neuron, 72*(5), 698-711. doi:10.1016/j.neuron.2011.11.003

Homberg, U., Hofer, S., Pfeiffer, K., & Gebhardt, S. (2003). Organization and neural connections of the anterior optic tubercle in the brain of the locust, *Schistocerca gregaria. The Journal of Comparative Neurology*, 462(4), 415-430.

Homberg, U., Heinze, S., Pfeiffer, K., Kinoshita, M., & el Jundi, B. (2011). Central neural coding of sky polarization in insects. *Philosophical Transactions of the Royal Society B: Biological Sciences, 366*(1565), 680-687. doi:10.1098/rstb.2010.0199

Ilieş, I., Muscedere, M. L., & Traniello, J. F. A. (2015). Neuroanatomical and morphological trait clusters in the ant genus *Pheidole*: evidence for modularity and integration in brain structure. *Brain, Behavior and Evolution, 85*(1), 63-76. doi:10.1159/000370100

Immonen, E. V., Dacke, M., Heinze, S., & El Jundi, B. (2017). Anatomical organization of the brain of a diurnal and a nocturnal dung beetle. *The Journal of Comparative Neurology, 525*(8), 1879-1908. doi:10.1002/cne.24169

Jayatilaka, P., Raderschall, C., Narendra, A., & Zeil, J. (2014). Individual foraging patterns of the jack jumper ant *Myrmecia croslandi* (*Hymenoptera: Formicidae)*. *Myrmecol. News, 19*, 75-83.

Krofczik, S., Khojasteh, U., de Ibarra, N., & Menzel, R. (2008). Adaptation of microglomerular complexes in the honeybee mushroom body lip to manipulations of behavioral maturation and sensory experience. *Developmental Neurobiology, 68*(8), 1007-1017. doi:10.1002/dneu.20640

Kubota, M., Tsuji, E., Misaka, Y., Yokohari, F., & Nishikawa, M. (2006). Polymorphism of brain neuropils in the carpenter ant, *Camponotus japonicus. Comparative Biochemistry and Physiology, Part B, 145,* 417-417.

Kühn-Bühlmann, S., & Wehner, R. (2006). Age-dependent and task-related volume changes in the mushroom bodies of visually guided desert ants, *Cataglyphis bicolor. Journal of Neurobiology, 66*(6), 511-521. doi:10.1002/neu.20235

Leitinger, G., Pabst, M. A., Rind, F. C., & Simmons, P. J. (2004). Differential expression of synapsin in visual neurons of the locust *Schistocerca gregaria*. *The Journal of Comparative Neurology, 480*(1), 89-100. doi:10.1002/cne.20333

Loesel, R., & Homberg, U. (2001). Anatomy and physiology of neurons with processes in the accessory medulla of the cockroach *Leucophaea maderae. The Journal of Comparative Neurology*, 439(2), 193-207. doi:10.1002/cne.1342

Maeda, T., Tamotsu, S., Iwasaki, M., Nisimura, T., Shimohigashi, M., Hojo, M. K., & Ozaki, M. (2014). Neuronal projections and putative interaction of multimodal inputs in the subesophageal ganglion in the blowfly, *Phormia regina*. *Chemical Senses, 39*, 391–401. doi:10.1093/chemse/bju007

Meyer, E., Matute, C., Streit, P., & Nässel, D. (1986). Insect optic lobe neurons identifiable with monoclonal antibodies to GABA. *Histochemistry, 84*(3), 207-216. doi:10.1007/BF00495784

Montgomery, S. H., & Ott, S. R. (2015). Brain composition in *Godyris zavaleta*, a diurnal butterfly, Reflects an increased reliance on olfactory information. *Journal of Comparative Neurology, 523*(6), 869-891. doi:10.1002/cne.23711

Muscedere, M., & Traniello, J. (2012). Division of labor in the hyperdiverse ant genus *Pheidole* is associated with distinct subcaste- and age-related patterns of worker brain organization. *PLoS ONE, 7*(2).

Nakadai, R., & Kawakita, A. (2017). Patterns of temporal and enemy niche use by a community of leaf cone moths (*Caloptilia*) coexisting on maples (*Acer*) as revealed by metabarcoding. *Molecular Ecology, 26*(12), 3309-3319. doi:10.1111/mec.14105

Narendra, A., Greiner, B., Ribi, W. A., & Zeil, J. (2016). Light and dark adaptation mechanisms in the compound eyes of *Myrmecia* ants that occupy discrete temporal niches. *The Journal of Experimental Biology, 219*(16), 2435-2442.

Narendra, A., Kamhi, J. F., & Ogawa, Y. (2017). Moving in dim light: behavioral and visual adaptations in nocturnal ants. *Integrative and Comparative Biology*. doi:10.1093/icb/icx096

Neuser, K., Triphan, T., Mronz, M., Poeck, B., & Strauss, R. (2008). Analysis of a spatial orientation memory in *Drosophila*. *Nature, 453*(7199), 1244-1247.

Niven, J. E., & Farris, S. M. (2012). Miniaturization of nervous systems and neurons. *Current Biology, 22*(9), R323-R329. doi:http://dx.doi.org/10.1016/j.cub.2012.04.002

Niven, J. E., & Laughlin, S. B. (2008). Energy limitation as a selective pressure on the evolution of sensory systems. *Journal of Experimental Biology, 211*(11), 1792.

Weir, P.T., & Dickinson, M. H. (2015). Functional divisions for visual processing in the central brain of flying *Drosophila*. *Proceedings of the National Academy of Sciences, 112*(40), E5523. doi:10.1073/pnas.1514415112

Ramirez-Esquivel, F., Zeil, J., & Narendra, A. (2014). The antennal sensory array of the nocturnal bull ant *Myrmecia pyriformi*s. *Arthropod Structure and Development, 43*(6), 543-558. doi:10.1016/j.asd.2014.07.004

R Core Team. (2017). R: A language and environment for statistical computing. Vienna, Austria: R Foundation for Statistical Computing. Retrieved from https://www.R-project.org/

Seelig, J. D., & Jayaraman, V. (2015). Neural dynamics for landmark orientation and angular path integration. *Nature, 521*(7551), 186-191. doi:10.1038/nature14446

Seid, M. A., Castillo, A., & Wcislo, W. T. (2011). The allometry of brain miniaturization in ants. *Brain, Behavior and Evolution, 77*(1), 5-13.

Seid, M. A., & Junge, E. (2016). Social isolation and brain development in the ant *Camponotus floridanus*. *The Science of Nature, 103*(5), 1-6. doi:10.1007/s00114-016-1364-1

Seid, M. A., & Wehner, R. (2008). Ultrastructure and synaptic differences of the boutons of the projection neurons between the lip and collar regions of the mushroom bodies in the ant, *Cataglyphis albicans*. *Journal of Comparative Neurology, 507*(1), 1102-1108. doi:10.1002/cne.21600

Stieb, S. M., Muenz, T. S., Wehner, R., & Rössler, W. (2010). Visual experience and age affect synaptic organization in the mushroom bodies of the desert ant *Cataglyphis fortis*. *Developmental Neurobiology, 70*(6), 408-423. doi:10.1002/dneu.20785

Schmitt, F., Stieb, S. M., Wehner, R., & Rössler, W. (2016). Experience-related reorganization of giant synapses in the lateral complex: Potential role in plasticity of the sky-compass pathway in the desert ant *Cataglyphis fortis. Developmental Neurobiology*, 76(4), 390-404. doi:10.1002/dneu.223221364-1

Stöckl, A., Heinze, S., Charalabidis, A., el Jundi, B., Warrant, E. J., & Kelber, A. (2016a). Differential investment in visual and olfactory brain areas reflects behavioural choices in hawk moths. *Scientific Reports, 6*, 26041. doi:10.1038/srep26041

Stöckl, A. L., O'Carroll, D. C., & Warrant, E. J. (2016b). Neural summation in the hawkmoth visual system extends the limits of vision in dim light. *Current Biology, 26*(6), 821-826. doi:10.1016/j.cub.2016.01.030

Stöckl, A. L., Ribi, W. A., & Warrant, E. J. (2016c). Adaptations for nocturnal and diurnal vision in the hawkmoth lamina. *Journal of Comparative Neurology, 524*(1), 160-175. doi:10.1002/cne.23832

Strauss, R. (2002). The central complex and the genetic dissection of locomotor behaviour. *Current Opinion in Neurobiology, 12*(6), 633-638.

Vacha, M. (2006). Laboratory behavioural assay of insect magnetoreception: magnetosensitivity of *Periplaneta americana*. *Journal of Experimental Biology, 209*(19), 3882-3886. doi:10.1242/jeb.02456

Varga, A. G., Kathman, N., Martin, J. P., Guo, P., & Ritzmann, R. (2017). Spatial navigation and the central complex: sensory acquisition, orientation, and motor control. *Frontiers in Behavioral Neuroscience, 11,* 4.

de Vries, L., Pfeiffer, K., Trebels, B., Adden, A., Green, K., Warrant, E.J., & Heinze, S. (2017). Comparison of navigation-related brain regions in migratory versus non-migratory Noctuid Moths. *Frontiers in Behavioral Neuroscience, 11,* 158 doi:10.3389/fnbeh.2017.00158

Warton, D. I., Wright, I. J., Falster, D. S., & Westoby, M. (2006). Bivariate line-fitting methods for allometry. *Biological Reviews, 81*(2), 259-291. doi:10.1017/S14647931060

Warton, D. I., Duursma, R. A., Falster, D. S., & Taskinen, S. (2012). smatr 3– an R package for estimation and inference about allometric lines. *Methods in Ecology and Evolution, 3*(2), 257-259. doi:10.1111/j.2041-210X.2011.00153.x

Wehner, R., Fukushi, T., & Isler, K. (2007). On being small: brain allometry in ants. *Brain, Behavior and Evolution, 69*(3), 220-228. doi:10.1159/000097057

Wei, H., el Jundi, B., Homberg, U., & Stengl, M. (2010). Implementation of pigment-dispersing factor-immunoreactive neurons in a standardized atlas of the brain of the cockroach *Leucophaea maderae. The Journal of Comparative Neurology, 518*(20), 4113-4133. doi:10.1002/cne.22471

Wolf, H. (2011). Odometry and insect navigation. *Journal of Experimental Biology, 214,* 1629-1641

Wystrach, A., Dewar, Alex, D. M., & Graham, P. (2014). Insect vision: emergence of pattern recognition from coarse encoding. *Current Biology, 24*(2), R78-R80. doi:10.1016/j.cub.2013.11.054

Figure Legends

Figure 1. Fig. 1 Whole brain micrographs of *M. gulosa* (**a**) and *M. midas* (**b**) with major brain neuropils labelled, outlined and colourised. Insets show the PB and NO of the CX

Figure 2. Activity patterns and head width distributions of *M. gulosa* and *M. midas*. (a) individual *M. gulosa* and *M. midas* workers (Photo credit: Ajay Narendra). (b) Activity pattern showing proportion of foragers exiting and entering the nest for both species over 24 hours. (c) Natural head width distributions and distributions of head widths of animals investigated in this study.

Figure 3. 3D reconstructions, scaling analyses and absolute volumes vs. head width for *M. gulosa* and *M. midas.* (a) Half views of the *M. gulosa* and *M. midas* brain in the dorsal (top), ventral (middle) and posterior (bottom) views. Animals were of near-identical body size and images are to the same scale. All neuropils labelled. (b) Standardised major axis (SMA) regressions of the total neuropil volumes against head width for both species.

Figure 4. Comparisons of the AL between *M. gulosa* and *M. midas*. Panel (a) shows the bull ant brain with the AL highlighted. Remaining neuropils transparent. Panel (b) shows the size of AL relative to the total volume of all brain neuropils in *M. gulosa* and *M. midas*. Panels (c) are plots of standardised major axis (SMA) regressions of the AL for *M. gulosa* and *M. midas.*

Figure 5. Comparisons of the OL between *M. gulosa* and *M. midas*. Panel (a) shows the bull ant brain with the OL highlighted. Remaining neuropils transparent. Panel (b) shows the size of OL relative to the total volume of all brain neuropils in *M. gulosa* and *M. midas*. Panels (c-f) are plots of standardised major axis (SMA) regressions of each region of the OL for *M. gulosa* and *M. midas.*

Figure 6. Comparisons of the MB between *M. gulosa* and *M. midas*. Panel (a) shows the bull ant brain with the MB highlighted. Remaining neuropils transparent. Panel (b) shows the size of MB relative to the total volume of all brain neuropils in *M. gulosa* and *M. midas*. Panels (c-g) are plots of standardised major axis (SMA) regressions of each region of the MB for *M. gulosa* and *M. midas.*

Figure 7. Comparisons of the CX between *M. gulosa* and *M. midas*. Panel (a) shows the bull ant brain with the CX highlighted. Remaining neuropils transparent. Panel (b) shows the size of CX relative to the total volume of all brain neuropils in *M. gulosa* and *M. midas*. Panels (c-

g) are plots of standardised major axis (SMA) regressions of each region of the CX for *M. gulosa* and *M. midas.*

Figure 1.

M. gulosa *M. midas*

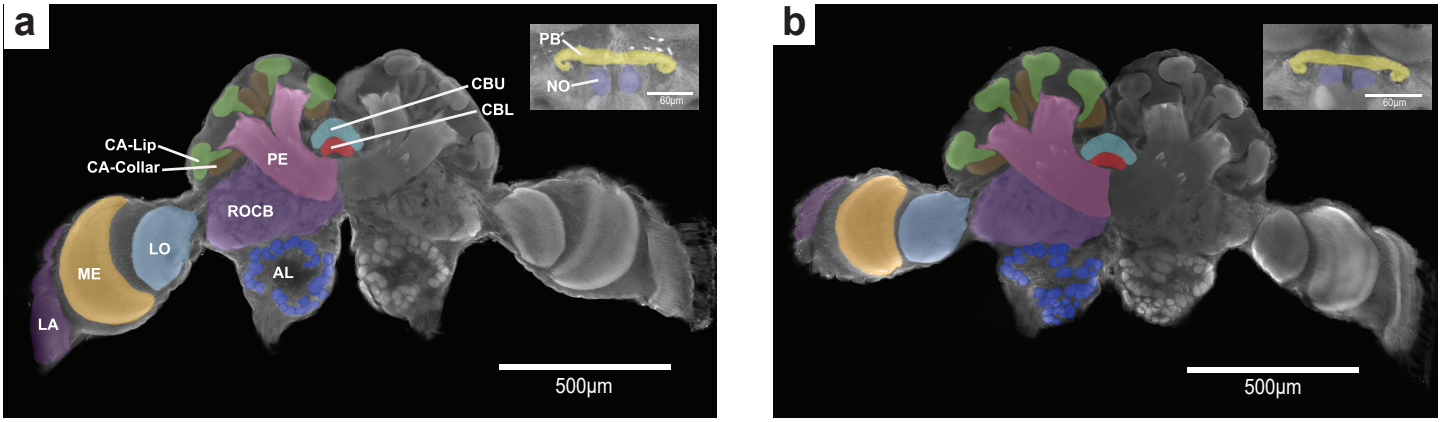

Figure. 2

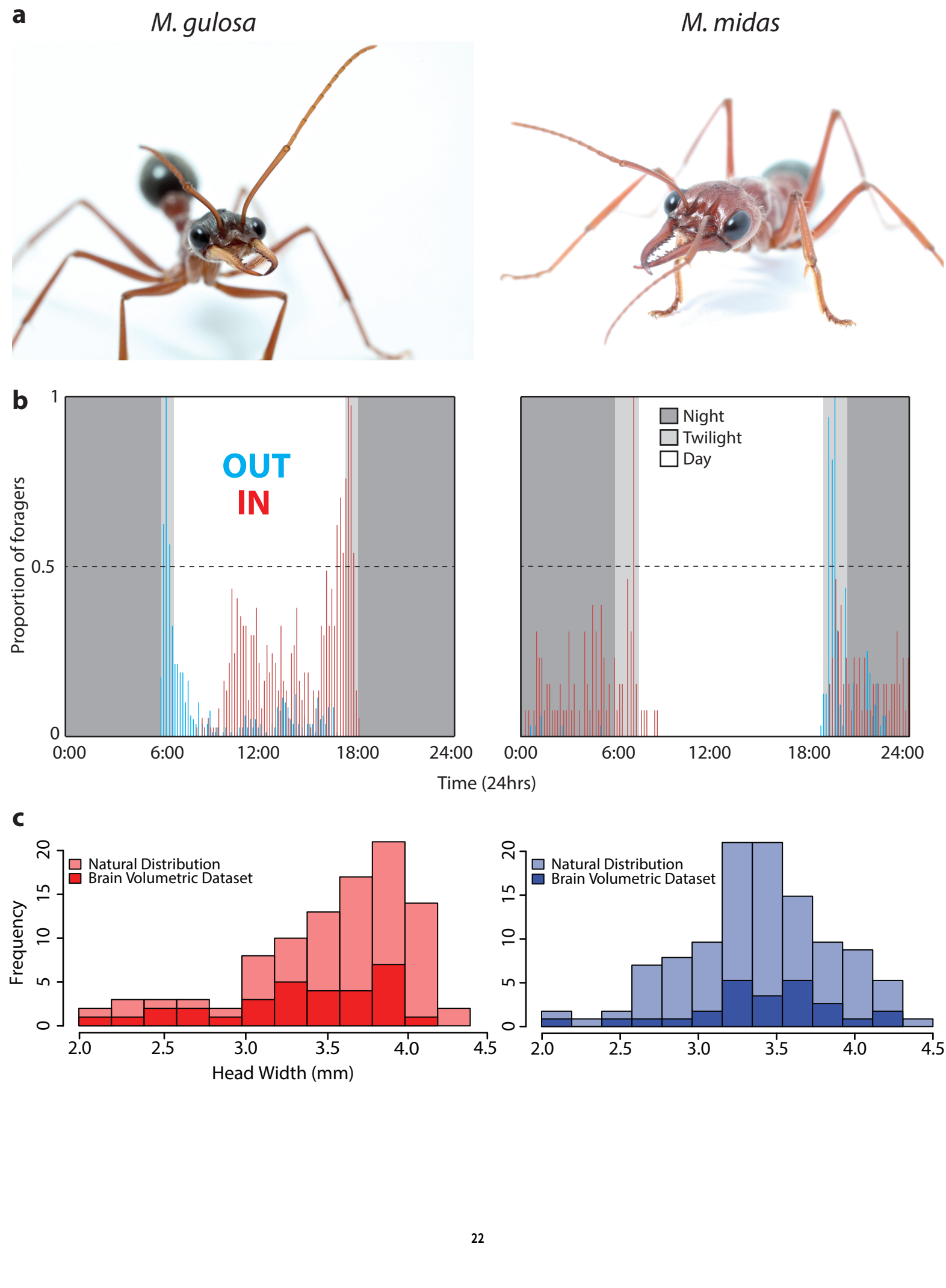
a
M. gulosa
M. midas
b
1
0.5
0
Proportion of foragers
OUT
IN
Night
Twilight
Day
0:00
6:00
12:00
18:00
24:00
Time (24hrs)
c
Natural Distribution
Brain Volumetric Dataset
Frequency
0
5
10
15
20
2.0
2.5
3.0
3.5
4.0
4.5
Head Width (mm)

Figure. 3

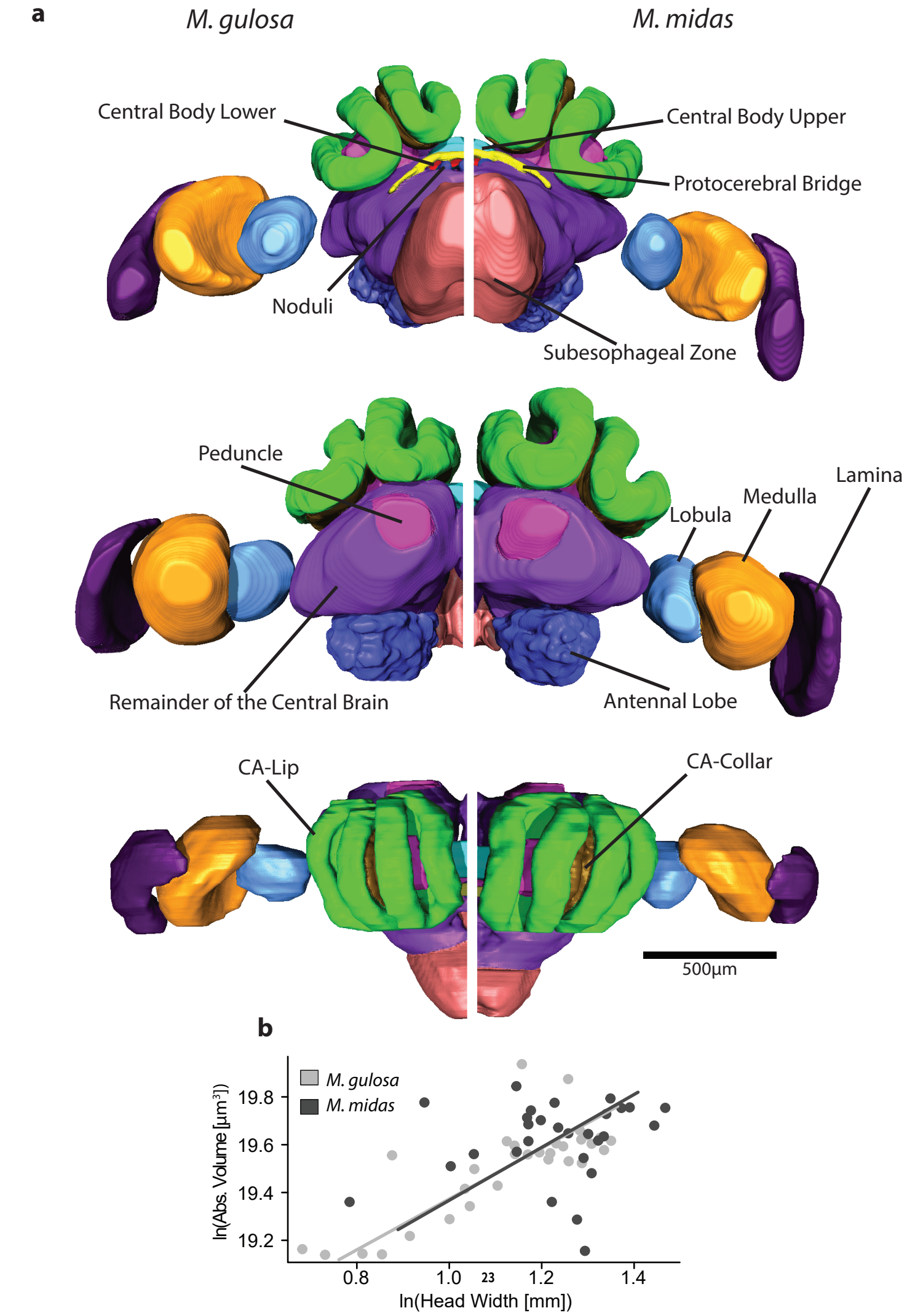
a
M. gulosa
M. midas
Central Body Lower
Central Body Upper
Protocerebral Bridge
Noduli
Subesophageal Zone
Peduncle
Lamina
Medulla
Lobula
Remainder of the Central Brain
Antennal Lobe
CA-Lip
CA-Collar
500µm
b
M. gulosa
M. midas
ln(Abs. Volume [µm³])
19.8
19.6
19.4
19.2
0.8
1.0
1.2
1.4
ln(Head Width [mm])

Figure. 4

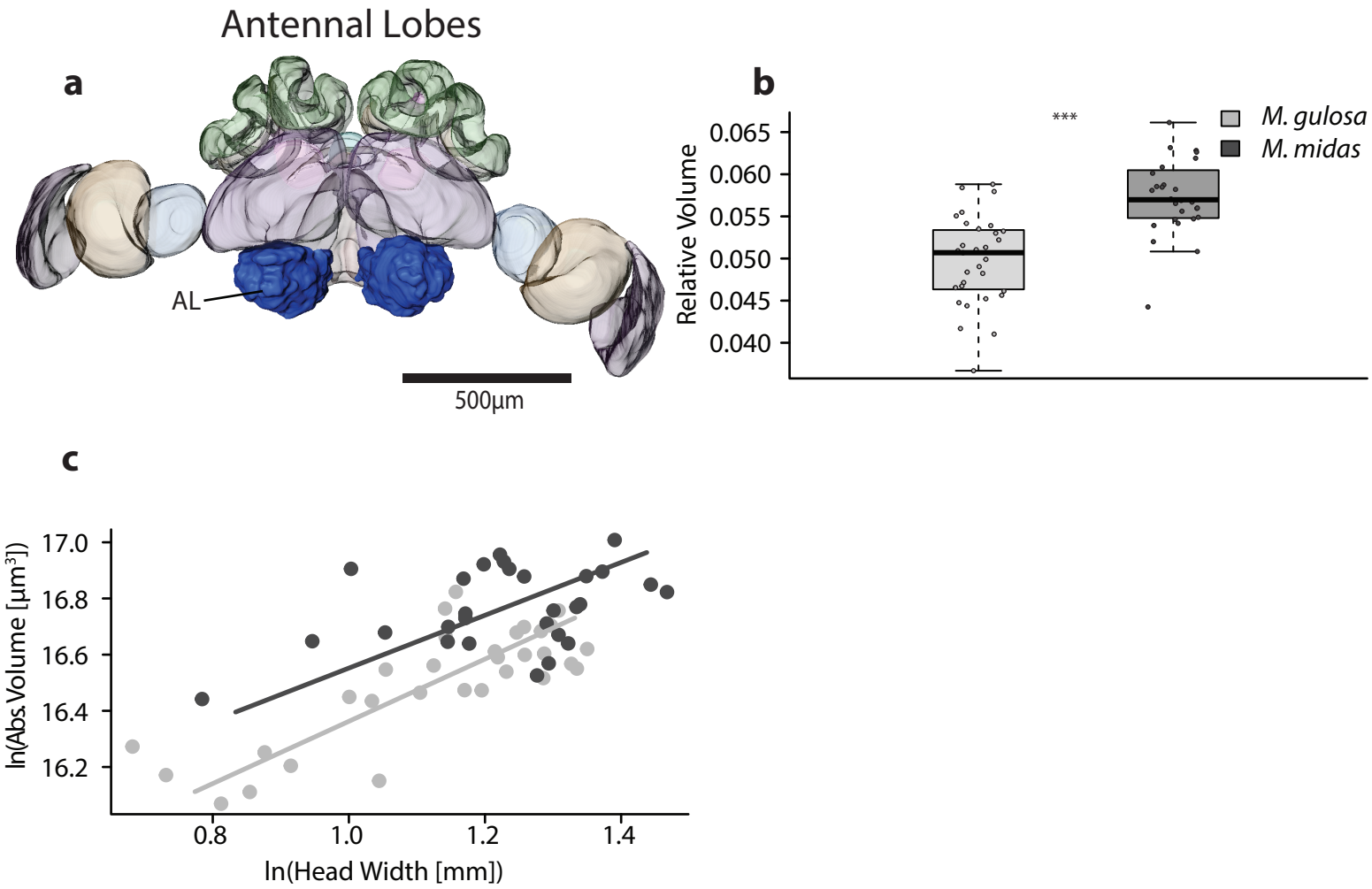
Antennal Lobes
a
AL
500µm
b
***
M. gulosa
M. midas
Relative Volume
0.065
0.060
0.055
0.050
0.045
0.040
c
ln(Abs.Volume [µm³])
17.0
16.8
16.6
16.4
16.2
0.8
1.0
1.2
1.4
ln(Head Width [mm])

Figure. 5

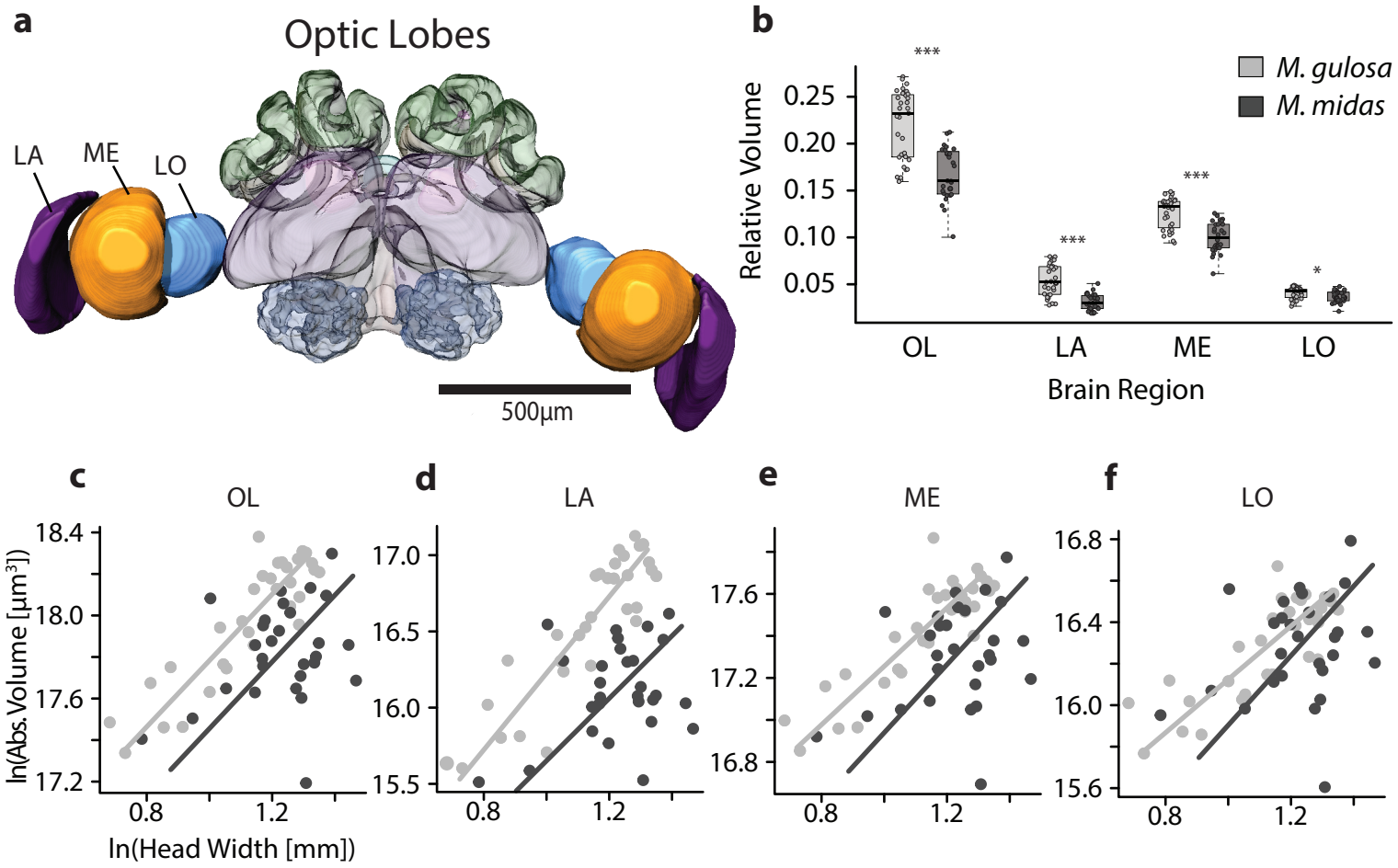
a
Optic Lobes
LA
ME
LO
500µm
b
M. gulosa
M. midas
Relative Volume
0.25
0.20
0.15
0.10
0.05
***
***
***
*
OL
LA
ME
LO
Brain Region
c
OL
d
LA
e
ME
f
LO
ln(Abs.Volume [µm³])
18.4
18.0
17.6
17.2
17.0
16.5
16.0
15.5
17.6
17.2
16.8
16.8
16.4
16.0
15.6
0.8
1.2
ln(Head Width [mm])

Figure. 6

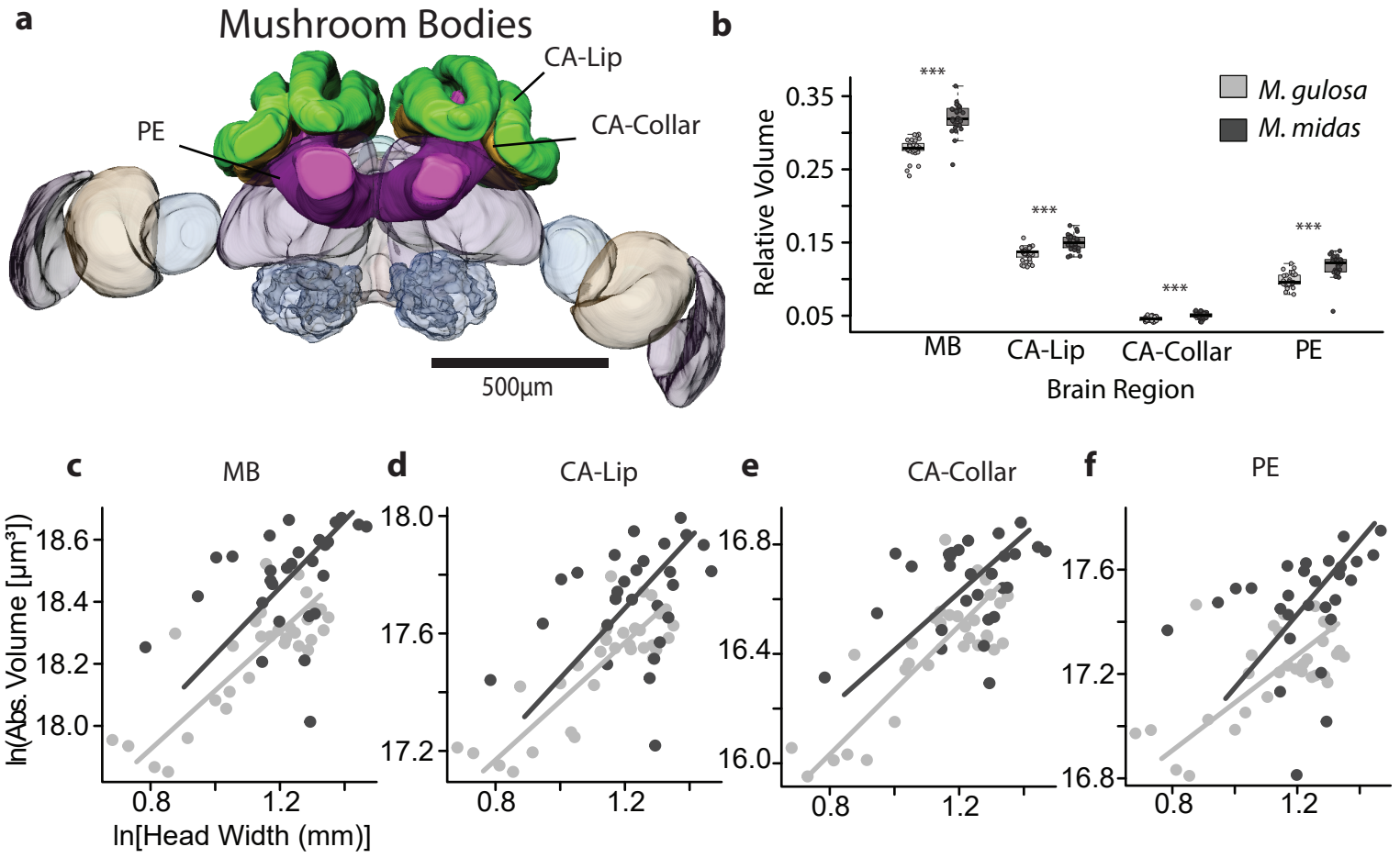
a
Mushroom Bodies
CA-Lip
PE
CA-Collar
500µm
b
Relative Volume
0.35
0.25
0.15
0.05
***
M. gulosa
M. midas
MB
CA-Lip
CA-Collar
PE
Brain Region
c
MB
d
CA-Lip
e
CA-Collar
f
PE
ln(Abs. Volume [µm³])
18.6
18.4
18.2
18.0
17.6
17.2
16.8
16.4
16.0
0.8
1.2
ln[Head Width (mm)]

Figure. 7

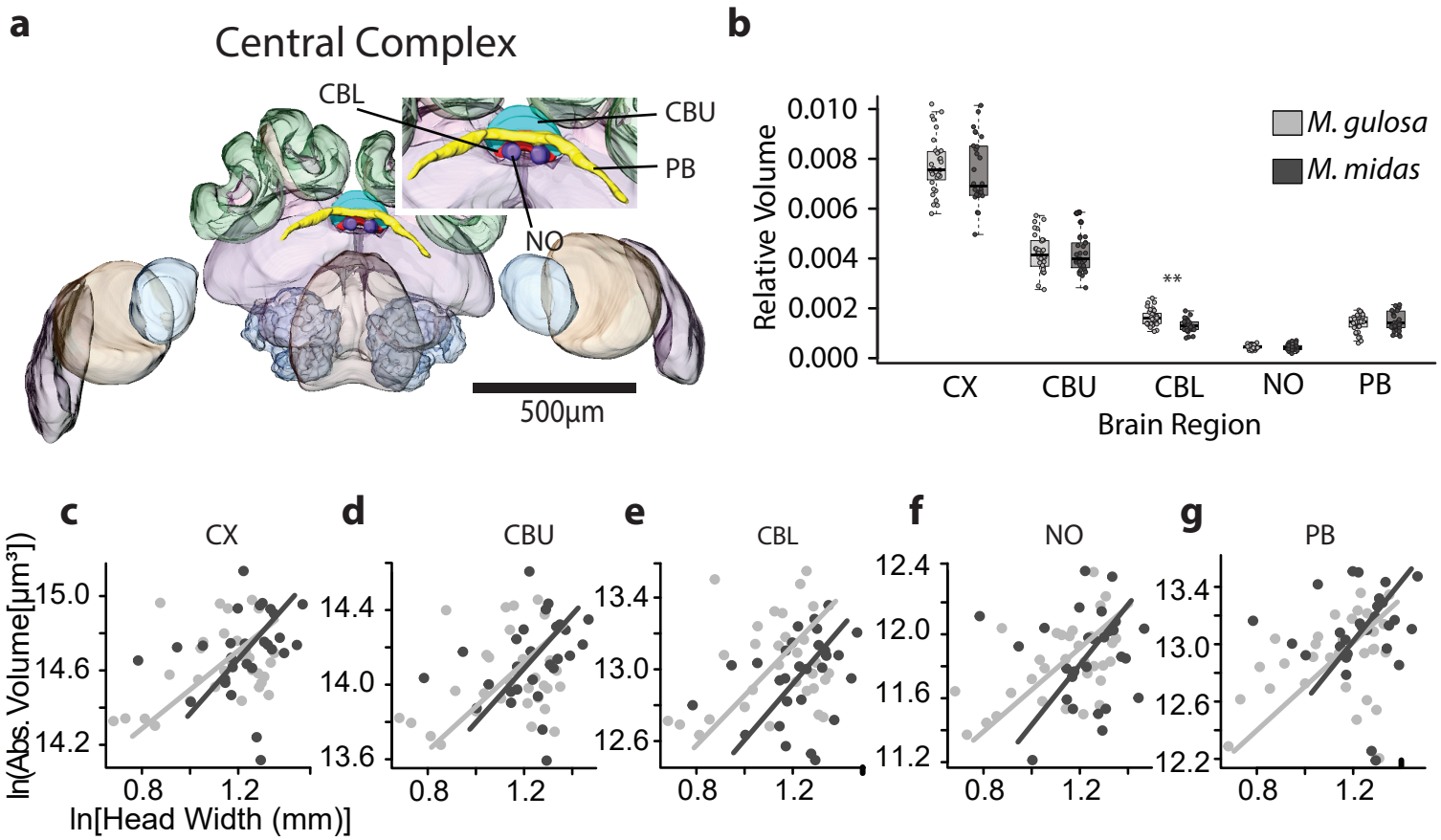
a
Central Complex
CBL
CBU
PB
NO
500µm
b
Relative Volume
0.010
0.008
0.006
0.004
0.002
0.000
**
M. gulosa
M. midas
CX
CBU
CBL
NO
PB
Brain Region

c
CX
d
CBU
e
CBL
f
NO
g
PB
ln(Abs. Volume[µm³])
15.0
14.6
14.2
14.4
14.0
13.6
13.4
13.0
12.6
12.4
12.0
11.6
11.2
12.2
0.8
1.2
ln[Head Width (mm)]

Supplementary Material

Table 1. Primary antibodies

Antigen	Immunogen	Manufacturer; species; clonality; Cat #; RRID	Dilution
Synapsin	Fusion protein of glutathione-S-transferase and the Drosophila SYN1 protein	Developed by G. Buchner (University of Würzburg, Germany), obtained from the Developmental Studies Hybridoma Bank, University of Iowa; mouse; monoclonal; Cat # 3C11 (anti SYNORF1); RRID: AB_528479	1:50

Table 2. Outputs of linear modelling investigating potential nest effects.

Region	Species	Multiple R^2	F-statistic	df	p-value
AL	*M. gulosa*	0.09575	0.6883	4, 26	0.6066
	M. midas	0.08801	0.5549	4, 23	0.6975
OL	*M. gulosa*	0.1434	1.089	4, 26	0.3827
	M. midas	0.287	2.314	4, 23	0.09793
MB	*M. gulosa*	0.1361	1.024	4, 26	0.4135
	M. midas	0.2327	2.867	4, 23	0.08602
CX	*M. gulosa*	0.1132	0.8294	4, 26	0.5186
	M. midas	0.0571	0.3482	4, 23	0.8425

Table 3. Outputs of t-tests comparing relative volumes of each brain region between species.

Functional Region	t-statistic	DF	p-value
AL	-5.7491	55.667	<0.0001
OL	6.3493	55.27	<0.0001
LA	6.7727	45.304	<0.0001
ME	6.1322	56.724	<0.0001
LO	2.6647	56.539	<0.01
MB	-8.7822	46.646	<0.0001
CA-Lip	-6.0711	53.238	<0.0001
CA-Collar	-6.7984	47.713	<0.0001
PE	-5.0134	47.713	<0.0001
CX	0.91497	53.352	0.4187
CBU	0.3829	56.387	0.7032
CBL	3.4022	56.064	0.00129
NO	0.7735	46.391	0.4431
PB	-0.94351	54.767	0.346

Table 4. Outputs of SMA regressions for each brain neuropil.

Region	Significantly different from 1?	Significant Grade shift?	Wald Statistic
Whole Brain	0.75609	0.94408	0.00492
AL	0.62641	0.00037832	12.64
OL	1.3741×10^{-6}	9.9095×10^{-7}	23.95
LA	4.3299×10^{-15}	1.5765×10^{-13}	54.47
ME	0.00018206	2.6637×10^{-5}	17.64
LO	0.0031164	0.03699	4.351
MB	0.81441	0.0015052	10.07
CA-Lip	0.67439	0.01529	5.883
CA-Collar	0.33949	0.01117	6.438
PE	0.18616	0.0066032	7.378
CX	0.14545	0.44591	0.581
CBU	0.10947	0.61269	0.2563
CBL	0.012692	0.0064207	7.428
NO	0.0020912	0.19098	1.71
PB	9.8486×10^{-5}	0.99415	5.369×10^{-5}

Table 5. R^2 and formula for scaling analysis of absolute volume against head width for each brain neuropil and for each species.

Functional Region	*M. gulosa*	*M. midas*	Common Slope
Whole Brain	y= 18.30953x + 1.0633445 R^2= 0.6249	y= 18.26054x + 1.1068450 R^2= 0.0415	y= 18.28964x + 1.0820675 R^2= 0.3655
AL	y= 15.25423x+ 1.1083651 R^2= 0.6423	y= 15.61148x+0.9406203 R^2= 0.0576	y= 15.15105x + 1.257218 R^2= 0.4133
OL	y=16.18685x + 1.596297 R^2= 0.7890	y= 15.84912x + 1.606429 R^2= 0.0238	y= 16.02686x + 1.601075 R^2= 0.2273
LA	y= 13.71199x + 2.514096 R^2= 0.7978	y= 13.60630x + 2.046114 R^2= 0.0563	y= 13.33490x + 2.560137 R^2= 0.1849
ME	y=15.86417x + 1.391371 R^2= 0.7699	y= 15.31862x + 1.620799 R^2= 0.0185	y= 15.65874x + 1.459687 R^2= 0.2137
LO	y= 14.83961x + 1.284664 R^2= 0.6647	y=14.22807x + 1.675658 R^2= 0.0077	y= 14.66557x + 1.379767 R^2= 0.2232
MB	y= 17.16787x + 0.9459800 R^2= 0.6479	y= 17.14710x + 1.0821776 R^2= 0.0175	y= 16.95968x + 1.182316 R^2= 0.3403
CA-Lip	y= 16.36993x + 0.9989042 R^2= 0.7077	y= 16.25534x + 1.1922873 R^2= 0.0039	y= 16.17632x + 1.2133101 R^2= 0.3295
CA-Collar	y= 15.09270x + 1.1748773 R^2= 0.6557	y= 15.36152x + 1.052572 R^2= 0.0427	y= 15.02616x + 1.279384 R^2= 0.4109
PE	y= 16.17426x + 0.9157196 R^2= 0.4022	y= 16.12003x + 1.1195678 R^2= 0.0227	y= 15.85808x + 1.263993 R^2= 0.2510
CX	y= 13.44769x + 1.0488888 R^2= 0.1483	y= 12.90327x + 1.4644666 R^2= 0.0440	y= 13.27120x + 1.1853792 R^2= 0.1124
CBU	y= 12.69845x + 1.1839606 R^2= 0.0661	y= 12.35201x + 1.4454388 R^2= 0.0520	y= 12.59568x + 1.261228 R^2= 0.0844
CBL	y= 11.46299x + 1.3909434 R^2= 0.0765	y= 11.04360x +1.562362 R^2= 0.1068	y= 11.34463x + 1.407333 R^2= 0.0577
NO	y= 10.347100x + 1.3055320 R^2=0.2623	y= 9.552076x + 1.881021 R^2= 0.0113	y= 10.096757x + 1.482994 R^2= 0.1091
PB	y= 11.16945x + 1.536443	y= 10.513778x + 2.089475	y= 10.91461x + 1.762863

	R^2= 0.1079	R^2=0.0038	R^2= 0.0755

Table 6. Outputs of linear modelling investigating influence of head width and species on variance for each brain neuropil.

Region	Model	Multiple R^2	F-statistic	df	p-value
Whole Brain	HW	0.2502	7.2	1, 57	$5.492x10^{-5}$
	Species	0.09044	5.668	1, 57	0.02064
	HW+ Species	0.2751	10.63	2, 56	0.0001224
AL	HW	0.3257	27.53	1, 57	$2.37x10^{-6}$
	Species	0.2913	0.2913	1, 57	$1.028x10^{-5}$
	HW+ Species	0.4748	25.32	2, 56	$1.473x10^{-8}$
OL	HW	0.2259	16.63	1, 57	0.0001425
	Species	0.1082	6.917	1, 57	0.01096
	HW+ Species	0.4703	24.86	2, 56	$1.875x10^{-8}$
LA	HW	0.1363	8.991	1, 57	0.004015
	Species	0.2766	21.8	1, 57	$1.887x10^{-5}$
	HW+ Species	0.5818	38.95	2, 56	$2.506x10^{-11}$
ME	HW	0.233	17.32	1, 57	0.0001079
	Species	0.06776	4.143	1, 57	0.04646
	HW+ Species	0.4135	19.74	2, 56	$3.255x10^{-7}$
LO	HW	0.2604	20.07	1, 57	$3.65x10^{-5}$
	Species	2.281e-05	0.0013	1, 57	0.9714
	HW+ Species	0.2846	11.14	2, 56	$8.472x10^{-5}$
MB	HW	0.3941	37.08	1, 57	$1.028x10^{-7}$
	Species	0.3779	34.63	1, 57	$2.22x10^{-7}$
	HW+ Species	0.5939	40.94	2, 56	$1.103x10^{-11}$
CA-Lip	HW	0.3902	36.47	1, 57	$1.24x10^{-7}$
	Species	0.3061	25.14	1, 57	$5.516x10^{-6}$
	HW+ Species	0.5372	32.5	2, 56	$4.273x10^{-10}$
CA-Collar	HW	0.4	38	1, 57	$7.729x10^{-8}$
	Species	0.3079	25.36	1, 57	$5.099x10^{-8}$
	HW+ Species	0.5465	33.74	2, 56	$2.428x10^{-10}$
PE	HW	0.2756	21.68	1, 57	$1.97x10^{-5}$
	Species	0.3735	33.98	1, 57	$2.733x10^{-7}$
	HW+ Species	0.5017	28.19	2, 56	$3.391x10^{-9}$
CX	HW	0.06475	3.946	1, 57	0.05179
	Species	0.035	2.067	1, 57	0.156
	HW+ Species	0.07822	2.376	2, 56	0.1022
CBU	HW	0.05651	3.414	1, 57	0.06985
	Species	0.04335	2.583	1, 57	0.1135
	HW+ Species	0.07709	2.339	2, 56	0.1058
CBL	HW	0.01804	1.047	1, 57	0.3105
	Species	0.02287	1.334	1, 57	0.2529
	HW+ Species	0.05836	1.735	2, 56	0.1857
PB	HW	0.04611	2.755	1, 57	0.1024

	Species	0.1092	6.989	1, 57	0.01057
	HW+ Species	0.1239	3.96	2, 56	0.02464
N	HW	0.07847	4.854	1, 57	0.03164
	Sp.	0.01046	0.6023	1, 57	0.4409
	HW+ Species	0.07884	2.396	2, 56	0.1003

Table 7. Slope Index (SI) for each of the neuropils investigated

Functional Region	Slope Index (SI)
Whole Brain	0.082067
AL	0.257218
OL	0.601075
LA	1.560137
ME	0.459687
LO	0.379767
MB	0.182316
CA-Lip	0.213311
CA-Collar	0.279384
PE	0.263993
CX	0.185379
CBL	0.261228
CBU	0.407333
NO	0.482994
PB	0.762863